UDK: 616.71:616.-079.3

CT AND MRI DIAGNOSTICS OF RHINO-ORBITO-CEREBRAL MUCORMYCOSIS IN PATIENTS WITH COVID-19

Abdashimov Zafar Bakhtiyarovich[1], Khodjibekova Yulduz Maratovna [2], Yunusova Lalita Rinatovna[2]
1 – Samarkand State Medical University, Republic of Uzbekistan, Samarkand;
2 – Tashkent State Dental Institute, Republic of Uzbekistan, Tashkent

COVID-19 БИЛАН ОҒРИГАН БЕМОРЛАРДА РИНООФТАЛЬМОЦЕРЕБРАЛ МУКОРМИКОЗ КТ ВА МРТ ДИАГНОСТИКАСИ

Абдашимов Зафар Бахтиярович[1], Ходжибекова Юлдуз Маратовна[2], Юнусова Лалита Ринатовна[2]
1 – Самарқанд давлат тиббиёт университети, Ўзбекистон Республикаси, Самарқанд ш.;
2 – Тошкент давлат стоматология институти, Ўзбекистон Республикаси, Тошкент ш.

КТ И МРТ ДИАГНОСТИКА РИНООФТАЛЬМОЦЕРЕБРАЛЬНОГО МУКОРМИКОЗА У ПАЦИЕНТОВ ПЕРЕНЕСШИХ COVID-19

Абдашимов Зафар Бахтиярович[1], Ходжибекова Юлдуз Маратовна[2], Юнусова Лалита Ринатовна[2]
1 – Самаркандский государственный медицинский университет, Республика Узбекистан, г. Самарканд;
2 – Ташкентский государственный стоматологический институт, Республика Узбекистан, г. Ташкент

e-mail: sammu@info.uz

Резюме. Риноофтальмоцеребрал мукормикоз (РОЦМ) эпидемик нисбатларда пайдо бўлди ва дунёда янги саломатлик муаммосини келтириб чиқарди. РОЦМ, ангиоинвазив инфекцияга Мucoraceae оиласининг филаментли замбуруғлари сабаб бўлади. Этиологик қилувчи омилларга қандли диабет, ўсма кассаликлари, аъзолар трансплантацияси, кортикостероидлардан фойдалниш ва иммунитет танқислиги ҳолати киради. Ўзбекистонда COVID-19 пандемияси даврида мукормикоз билан касалланганлар сони сезиларли даражада ошди. Мукормикоз асосан қандли диабет беморларда кузатилади, уларда COVID-19 инфекцияси асоратлар ва ўлим хавфини оширади. Компьютер томографияси (КТ) РОЦМда нисбатан камроқ рол ўйнайди, магнит-резонанс томография (МРТ) кўра, бу касалликнинг кенгайишини баҳолаш учун юмшоқ тўқималарнинг умумий резолюциясига эга.

Калит сўзлар: Риноофтальмоцеребрал мукормикоз, КТ, МРТ, COVID-19.

Abstract. Rhino-orbito-cerebral mucormycosis (ROCM) has emerged in epidemic proportions, triggering a new health challenge in world. ROCM, an angioinvasive infection, is caused by the filamentous fungi of the family of Mucoraceae. Predisposing factors include uncontrolled diabetes, hematologic malignancies, solid-organ and stem cell transplantations, use of corticosteroids, and an immunocompromised status. There has been a substantial rise in the number of patients with mucormycosis in Uzbekistan during the COVID-19 pandemic. ROCM is predominantly seen in patients with diabetes/prediabetes in whom COVID-19 infection increases the risk of complications and fatality. Computed tomography (CT) in ROCM has a relatively lesser role as compared with magnetic resonance imaging (MRI), which has overall better soft-tissue resolution to assess disease extension.

Keywords: Rhino-orbito-cerebral mucormycosis, CT, MRI, COVID-19.

Introduction. Rhino-orbito-cerebral mucormycosis (ROCM) has emerged in epidemic proportions, triggering a new health challenge in world. ROCM, an angioinvasive infection, is caused by the filamentous fungi of the family of Mucoraceae. Multiple determinants of ROCM in the background of COVID-19 have been proposed. Pre-disposing factors include uncontrolled diabetes, hematologic malignancies, solid-organ and stem cell transplantations, use of corticosteroids, and an immunocompromised status [1]. There has been a substantial rise in the number of patients with mucormycosis in Uzbekistan during the COVID-19 pandemic. The combination of the novel severe acute

respiratory syndrome coronavirus 2 infection along with early and overuse of steroids/monoclonal antibodies and broad-spectrum antibiotics may be the prime factors for the conditions resulting in immune dysregulation[2]. ROCM is predominantly seen in patients with diabetes/prediabetes in whom COVID-19 infection increases the risk of complications and fatality [2]. The pathogenesis of the development of mucormycosis in COVID-19 infection is multifactorial. Clinical features include nasal stuffiness, epistaxis, nasal discharge, swelling of the face, facial and/or orbital pain, worsening headache, proptosis, sudden loss of vision, facial paresthesia, sudden ptosis, diplopia, facial palsy, fever, paralysis, and focal seizures. Early detection and treatment are crucial to improving outcome, which is highlighted by worse clinical outcomes in subjects with higher imaging stages. Computed tomography (CT) in ROCM has a relatively lesser role as compared with magnetic resonance imaging (MRI), which has overall better soft-tissue resolution to assess disease extension.

Contrast-enhanced MRI plays a vital role in both diagnosis and prognostication. Because of superior spatial resolution and softtissue contrast, MRI is the preferred imaging modality to evaluate intraorbital extension, skull base extension, meningeal involvement, brain parenchymal involvement, perineural, and angioinvasion. Recently, Mazzai et al. [3] elaborated a pictorial review of mucormycosis from onset to vascular complications, putting forth a 3-stage grading system of involvement. In summary, the 3 stages in progressive increments of involvement include sinonasal, orbital, and intracranial involvement. From this multi-institutional study, we intend to highlight the radiologic imaging patterns of ROCM that are associated with COVID-19. As a secondary end point, we aim to seek possible associations with other clinicodemographic variables.

Materials and methods. This is a retrospective imaging study of 101 patients who were diagnosed with COVID-19 associated with mucormycosis by histopathology and/or culture. Institutional approval was obtained for the collection of imaging and basic clinical data.

All patients underwent CT and/or MRI with or without contrast, based on the clinical condition of the patient and on consensus decision by the team of treating physicians. Imaging was evaluated and staged by 2 experienced neuroradiologists independently. The imaging protocol is discussed in Table 1.

Patients either had active COVID-19 infection or had recently recovered from COVID-19 infection with an interval period of 3-30 days. Cases were pooled from 4 different tertiary care centers in the world, during the second wave of COVID-19 in the month of May 2021. Apart from imaging, other essential clinical details also were collected, including the status of diabetes, administration of steroids or other immune modulators such as tocilizumab, supplementary oxygen, the interval between COVID-19 and diagnosis of mucormycosis, treatment, and outcome. A simple 3-stage classification system was adopted. The proposed staging system was adapted from Mazzai et al. [4] and modified for detailed analysis (Table 2).

Data collection and imaging details of the staging were shared with the participating institutions for maintaining uniformity of collected data (Table 3).

Data were collected on an Excel spreadsheet (Microsoft, Redmond, Washington, USA). Statistical analysis was performed on R software (version 3.1.3; The R Foundation for Statistical Computing, Vienna, Austria). KruskaleWallis nonparametric test was employed for group comparison of continuous variables. The 2 test was used for ordinal variables.

Table 1. Imaging Protocol in Suspected Cases of Mucormycosis.

ROCM-Imaging Techniques	
CT of the brain, orbits, and PNS	MRI of the brain, orbits, and PNS
Vertex to mandible with contrast	Axial FLAIR, DWI, SWI of brain
Assessment of	T1WI and T2WI orbit/PNS in at least 2 planes (3-mm fat-suppressed)
- Sinus contents	Postcontrast T1WI 3D axial brain
- Bone erosion or osteomyelitis	Postcontrast FS T1WI orbit/PNS
- Perisinus or orbital invasion	Superior for assessment of soft tissue, perineural, vascular, and brain invasion
- Brain lesions (infarct, vasogenic edema, hemorrhage or abscess)	Scan duration w25 minutes.
CT angiogram- If thrombus or pseudoaneurysm (mycotic) is suspected	
CT may under stage extent of disease	

ROCM, rhino-orbital-cerebral mucormycosis; CT, computed tomography; PNS, paranasal sinuses; MRI, magnetic resonance imaging; FLAIR, fluid-attenuated inversion recovery; DWI, diffusionweighted imaging; SWI, susceptibility-weighted imaging; WI, weighted imaging; 3D, 3-dimensional; FS, fat-suppressed.

Table 2. Proposed 3-Tier Staging of ROCM

Stage 1: Sinonasal involvement	1A: Involvement of 1 sinus and ipsilateral middle turbinate.
	1B: Involvement of >1 ipsilateral sinus and/or turbinate
	1C: Involvement of bilateral sinonasal cavities.
Stage 2: Orbital involvement	2A: Involvement of medial and/or inferior orbital compartment only.
	2B: Diffuse unilateral orbital involvement with or without optic nerve, nasolacrimal duct, and vascular involvement.
	2C: Bilateral orbital involvement.
Stage 3: Central nervous system involvement	3A: Involvement of pachymeninges, cribriform plate, cavernous sinus/Meckel's cave.
	3B: Vascular involvement (infarct/bleed)/perineural spread and skull base involvement.
	3C: Leptomeningitis, cerebritis or abscess formation - focal or diffuse involvement.

ROCM, rhino-orbital-cerebral mucormycosis

Table 3. Key Imaging Findings to be Assessed and Documented

Stage 1: Look for specific signs of invasive sinusitis apart from nonspecific mucosal thickening or collection such as
Periantral loss of fat planes or stranding
Lack of sinus mucosal enhancement (LOE)
Lack of turbinate enhancement (black turbinate)
Involvement of nasal septum/palate (perforation and LOE)
Look for pterygopalatine fossa (PPF) involvement
Stage 2: Look for specific signs of invasive sinusitis extending to orbits such as
Bony erosions (CT)
Orbital fat stranding (dirty fat sign on T2-FS)
Look for features of early involvement of medial orbital wall and extraocular muscles
In case of vision loss, look for optic nerve ischemic infarct (DWI-restricted diffusion)
Look for Involvement of orbital apex and fissures
Look for perioptic sheath, sclera and globe morphology
Look for loss of flow void &and enhancement in the superior ophthalmic vein (If enlarged, then rule out cavernous sinus thrombosis)
Bony erosions (CT)
Stage 3: Look for specific signs of invasive sinusitis extending to CNS such as Cavernous sinus and Meckel's cave involvement (enlargement and LOE)
Look for signs of carotid artery narrowing or thrombosis or pseudoaneurysm formation
Look for features of cranial nerve thickening especially, trigeminal nerve
Look for meningeal thickening and enhancement in ACF and MCF
Look for skull base involvement in T2-FS and PC-T1FS thin sections
Look for cerebritis or abscess or infarcts or subarachnoid hemorrhage
Bony erosions (CT)

CT, computed tomography; T2-FS, T2-weighted fat-suppressed; DWI, diffusion-weighted imaging; CNS, central nervous system; ACF, anterior cranial fossa; MCF, middle cranial fossa; PC-T1FS, postcontrast T1-weighted fat-saturated images.

Results. One hundred one cases were included in the final analysis (Mean age ¼ 55.1 years; range ¼ 26-85 years; male/female ratio ¼ 67:34; stage 1, n ¼ 18; stage 2, n ¼ 39; stage 3, n ¼ 44; Supplementary Figure 1). The patient population had known diabetes in 94% of the instances (n ¼ 95). Systemic steroids had been administered in 80.1% (n ¼ 81), whereas 59.4% (n ¼ 60) of patients received supplemental oxygen. Eleven subjects had been advised to isolate at home. The majority underwent surgical intervention, whereas only 6 cases were treated solely with antibiotic regimens. Sixty subjects showed clinical improvement to therapy, whereas 18 eventually succumbed to the illness.

The mean age of the patients across the imaging stages (1e3) was 59.7 _ 10.7, 55.3 _ 13.3, and 53.0 _ 11.0 years, respectively. No statistical difference was seen in the mean age across the groups of patients (stages 1-3) (P ¼ 0.18).
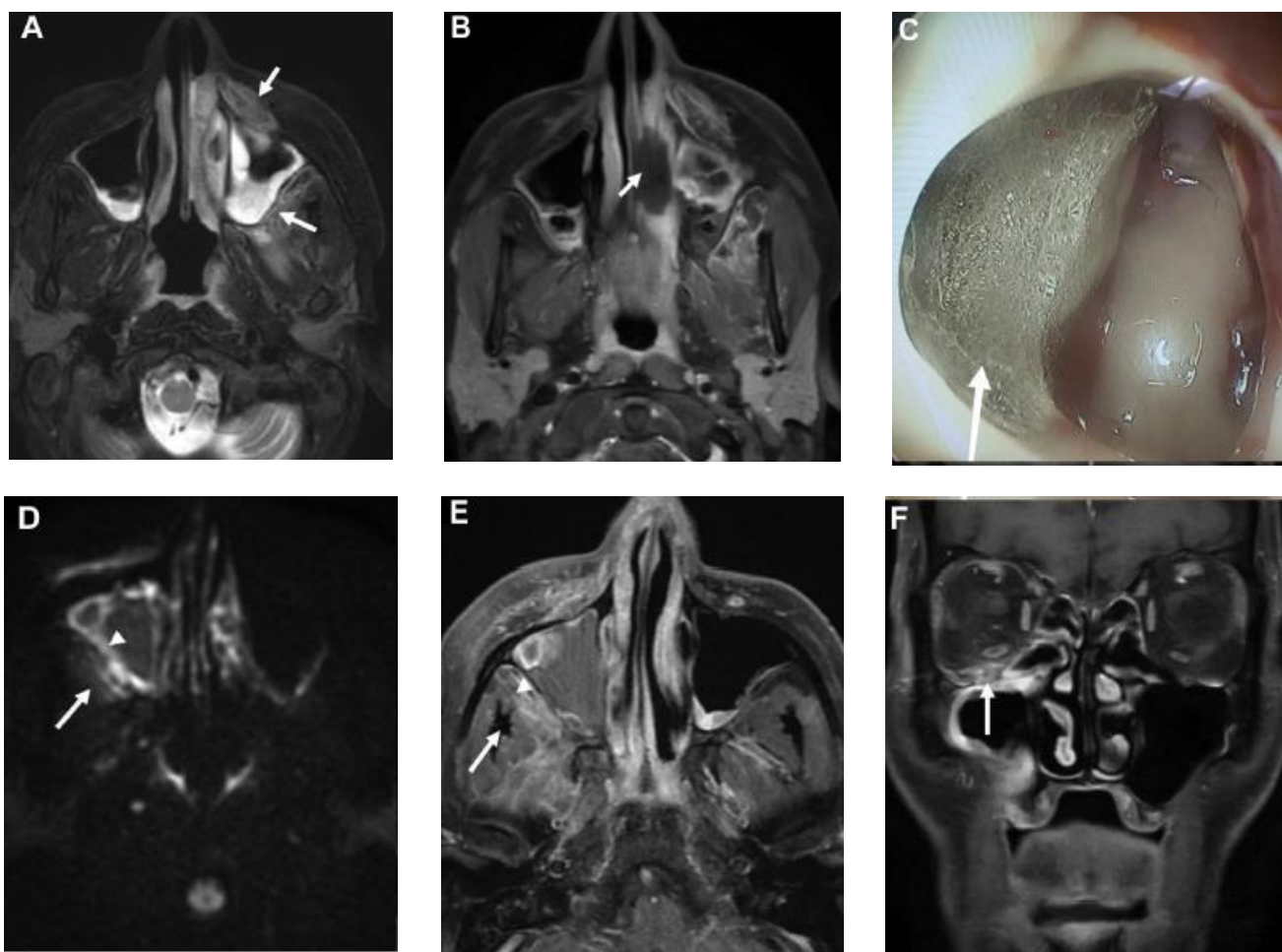
Figure 1. Key imaging features of stage 1 disease. A 65-year-old man, status 21 days' post-coronavirus disease 2019 (COVID-19), presented with facial pain and numbness over 5 days. He was treated and discharged 7 days back from the hospital for moderate COVID-19 pneumonia with a computed tomography (CT) severity score of 15 of 25. The second row is from another patient with similar clinical profile with right-sided paranasal sinus involvement. (A) Axial T2-weighted fat-suppressed image showing early signs of stage 1 rhino-orbital-cerebral mucormycosis. Hyperintensity in the left premaxillary and retroantral region with represents periantral inflammation (arrows). Note the bilateral maxillary sinusitis. (B) Axial T1-weighted (T1W) fat-saturated postcontrast image showing focal area of nonenhancement of the inferior turbinate suggesting necrosis (arrows), the so-called "black turbinate" sign. (C) Nasal endoscopy image depicting fungal colony in the maxillary antrum (arrow). (D) Axial diffusion-weighted image showing bright signal along lateral mucosal wall of right maxillary sinus (arrowhead) and in the retroantral soft tissue (arrow). (E) Axial T1W fat-saturated postcontrast image shows focal lack of enhancement in the lateral wall mucosa of right maxillary sinus (arrowhead) and enhancing retroantral soft tissue (arrow). (F) Coronal T1W fat-saturated postcontrast image shows enhancement along the right infraorbital nerve within the infraorbital foramen suggesting early perineural spread of the disease (arrow). Note the right maxillary sinus mucosal thickening and adjoining orbital fat stranding.

Sex predisposition to worse clinical outcomes (P ¼ 0.78) or imaging stages (P ¼ 0.96) was not observed. No statistically significant difference was noted in the mean duration (in days) between the diagnosis of COVID-19 and ROCM across the 3 imaging subgroups of patients (15.4 _ 8.9, 14.3 _ 7.0, 16.0 _ 7.0 for stages 1e3, respectively; P ¼ 0.86). KruskaleWallis nonparametric test revealed no significant association of steroid use (P ¼ 0.53), diabetes (P ¼ 0.74), or oxygen supplementation (P ¼ 0.12) with higher imaging stages, neither was an association discernible between the aforementioned variables and clinical outcomes. As hypothesized, there was a significant correlation of higher imaging stages with poor clinical outcomes (P ¼ 0.0003). Table 4 summarizes the prevalence of key imaging findings, and Figures 1-5 represent the important imaging findings, respectively.

Discussion. In this study, we present a series of patients who developed ROCM in the background of COVID-19 infection.

Disease severity ranged from isolated involvement of sinuses to extensive involvement of the brain. Disease severity on imaging showed a correlation with the clinical outcomes. The purported disease-modifying variables, such as diabetes and use of steroids, which have been identified in previous works, were noted with a similar preponderance in our study [4]. The mean age of the patients was relatively high, with a male preponderance.

Table 4. Prevalence of Key Imaging Findings

| Imaging Finding/Involved Structure	Prevalence
Lack of sinonasal mucosal enhancement (including "black turbinate" sign)	87 (86%)
Perisinus inflammation	101 (100%)
Orbital apex	33 (33%)
Ischemic optic neuropathy	12 (11.8%)
Skull base involvement	25 (24.7%)
Cavernous sinus/pachymeningeal involvement	32 (31.6%)
Meckel's cave involvement	26 (25.7%)
Leptomeningitis	17 (16.8%)
Cerebritis	12 (11.8%)
Intracerebral abscess	5 (4.9%)
Perineural spread	29 (28.7%)
Ischemic stroke	10 (10%)
Subarachnoid hemorrhageeaneurysmal rupture	2 (1.9%)
Extension of the infective process along the fifth nerve into the brainstem	1 (1%)
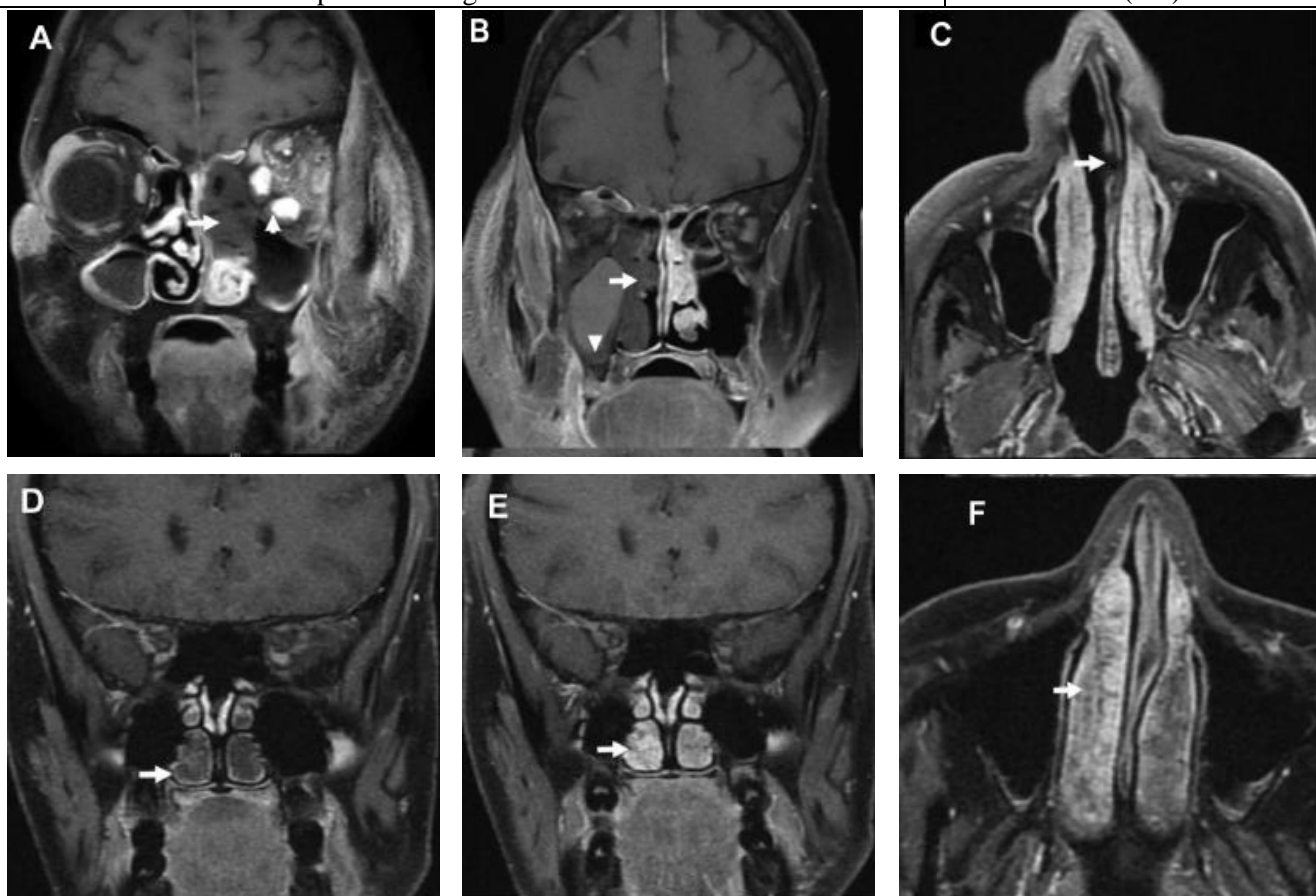
Figure 2. Key imaging features in from 3 different patients showing varying degree of nasal turbinate and nasal septum involvement. All 3 patients had recovered from COVID-19 and were readmitted between 7 and 21 days. The top row is showing representative cases of the "black turbinate" sign (AeB) and nasal septal involvement (C), and the bottom row is representing benign turbinate hypertrophy from control patients outside the study cohort (DeF). (A) Coronal T1-weighted (T1W) fat-saturated postcontrast image shows complete lack of enhancement involving left-sided turbinates representing the "black turbinate" sign (arrows). Also note extension to ipsilateral orbit (arrowhead) and extensive soft-tissue inflammation in the right infratemporal fossa (arrowheads). (B) Coronal T1W fat-saturated postcontrast image shows complete lack of enhancement involving right-sided turbinates representing the "black turbinate" sign (arrows) Also note the lack of mucosal enhancement in the ipsilateral maxillary sinus (arrow) and extensive soft tissue inflammation in the left infratemporal fossa (arrowheads). (C) Axial T1W fat-suppressed postcontrast image showing nasal septal perforation (arrows). (D) Coronal T1W fat-saturated postcontrast image showing preserved enhancing mucosal lining (arrow). (E) Coronal T1W fat-saturated 5 minutes' delayed postcontrast image showing progressive complete enhancement of turbinates (arrow). (F) Axial T1W fat-saturated postcontrast images showfeatures of normal turbinates like fine internal striations/septae (arrow).
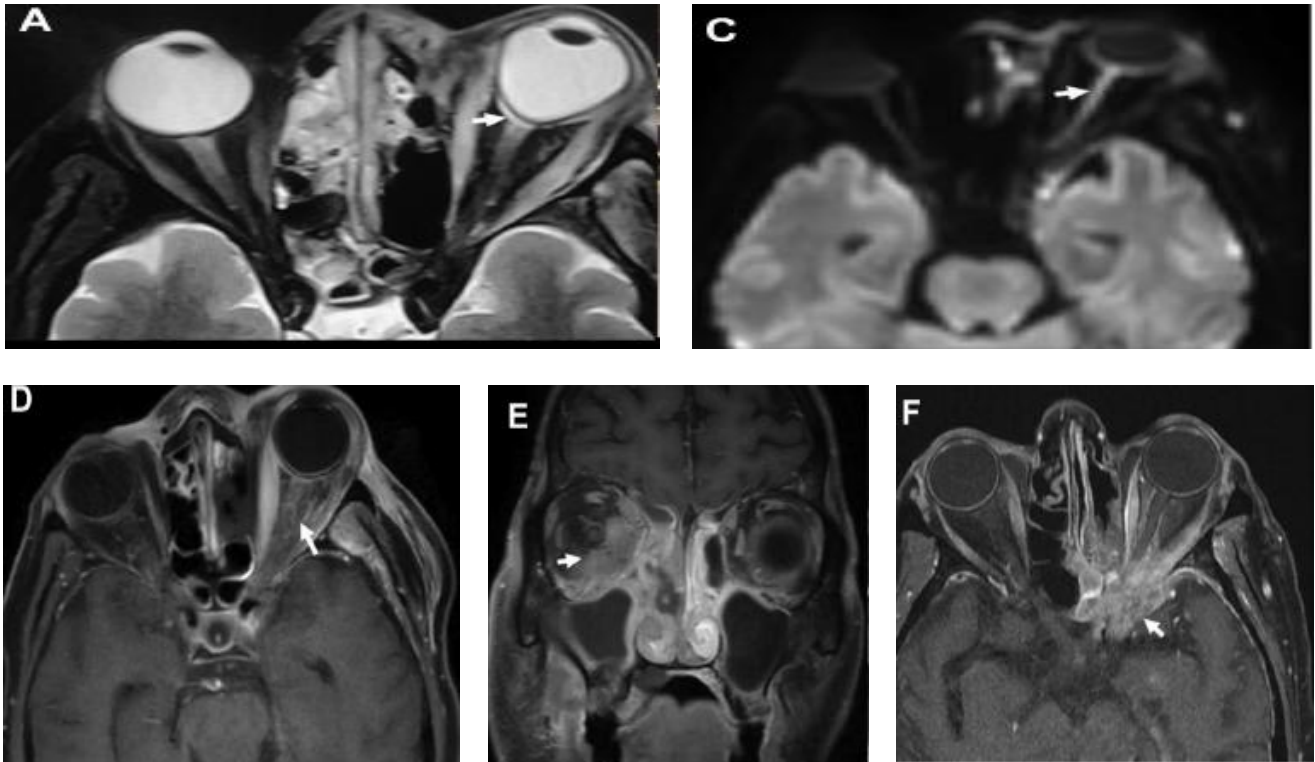
Figure 3. Key imaging features in stage 2 disease from 4 different patients showing varying degrees of orbital involvement. All 4 patients had recovered from coronavirus disease 2020 (COVID-19) and were readmitted between days 7 and 18. All had diabetes, with only 2 receiving both steroids and supplementary oxygen during COVID-19 illness. (AeB) Axial T2-weighted fat-suppressed image showing left posterior ocular globe tenting (arrow) similar to the shape of a guitar pick, indicating increased intraorbital pressure. (C) Axial diffusion-weighted image showing bright signal along the right optic nerve (arrow) indicating acute optic nerve ischemia. (D) Axial T1-weighted (T1W) fat-saturated postcontrast image shows thickened and enhancing entire left optic nerve and optic sheath with surrounding fat stranding (arrow). (E) Coronal T1W fat-saturated postcontrast image shows enhancing retro-orbital soft tissue along the medial and inferior aspects (bulky extraocular muscles) of right orbit (arrow). (F) Axial T1W fat-saturated postcontrast image depicts irregular enhancing soft tissue at the region of left orbital apex (arrow). Note the adjacent left sphenoid sinus involvement and postoperative changes in the ipsilateral ethmoids.

The demographic characteristics that we report in terms of the age group and sex distribution of the subject population of our study are similar to that noted in the recent past in the subcontinent [5]. No other significant association was noted between any of the clinical variables and imaging stages and clinical outcomes. Most patients in the series were managed surgically, and 18 patients eventually succumbed to their illness. The imaging features that correlate to the clinical outcomes can be elucidated by the 3-stage system adapted in the study for prudent clinical decision-making. It is to be noted that this system also takes into account the pathogenetic mechanisms involved in the progression. In stage 1, the disease is characterized by the involvement of the nasal cavity and paranasal sinuses (Table 3). Early signs of invasive sinusitis are periantral loss of fat planes and lack of enhancement involving turbinates, nasal septum, and palate. Lack of normal turbinate enhancement on contrast study is called the "black turbinate" sign and indicates tissue infarction [6]. It needs to be distinguished from benign turbinate hy-

pertrophy, which shows mucosal enhancement in immediate scan followed by progressive complete enhancement on delayed images [7].

Nonenhancing mucosal thickening with diffusion restriction is another important early indicator of the disease. Fungal elements within the paranasal sinuses are seen as T2 hypointensity due to iron and other minerals contrary to the hyperintense signal on bland mucosal thickening [8]. The pterygopalatine fossa has extensive connections with the deep face and sinuses and its involvement facilitates extension to the deep neck tissues, orbit and brain. Secondary cutaneous mucormycosis shows inflammatory changes in the facial soft tissue as seen in most of our cases. Subtle signs of bony erosion may be seen on CT but during the early disease stage, it may be completely normal. In stage 2, the orbital compartment is involved with the spread of disease to extraocular muscles and retroorbital fat with the formation of subperiosteal collection in some patients. Narrowing of the posterior globe angle to less than 130_ is called globe tenting or "guitar pick sign," and it indicates

raised intraorbital tension caused by the ongoing retrobulbar inflammation and consequent orbital compartment syndrome [9]. This is not specific for ROCM but indicates poor visual prognosis [10]. As the disease progress, other findings like optic nerve sheath thickening, involvement of orbital fissures, orbital apex and enlarged superior ophthalmic vein with or without thrombosis may be noted. In case of vision loss, diffusion restriction of the optic nerve may be seen which indicates optic nerve ischemia, and it is another indicator of poor outcome.

Skull base and central nervous system involvement suggest stage 3 disease. Focal pachymeningeal thickening and enhancement mainly involving anterior and middle cranial fossa along the anteroinferior temporal convexity and lateral wall of the cavernous sinus and tentorium cerebelli may be seen. Skull base osteomyelitis is seen as bone marrow edema and bone erosions. Perineural invasion seen in a significant number of cases in our study cohort may be an under-recognized entity. Extension to the nerves via vasa nervorum is a possibility, and more recent studies have shown high affinity of mucor to epithelial growth factor receptor and extracellular matrices in basement membranes, specifically laminin and type 4 collagen and both are abundant in peripheral nerves [11]. Perineural invasion also is determined by the nerve microenvironment and neurotrophic elements secreted along the nerves[12]. Perineural spread is seen as enlargement and variable enhancement of the cranial nerves, especially the trigeminal nerve either in the cisternal portion or within the foramen or canal [13]. The disease also may spread directly into the anterior cranial fossa through the cribriform plate. Meckel's cave involvement is demonstrated distinctly on T2-weighted imaging as hypointense or dirty signal intensity. Isolated sixth cranial nerve palsy in the absence of other cranial neuropathies suggests a predominant skull base infective process [14]. The greater (43.54%) composition of stage 3 that we note in this study may likely pertain to referral bias or may be due to the smaller number of patients included in the previous studies due to the relative rarity of the mucor infection. The greater likelihood of poor outcomes associated with intracranial extension implies that meticulous efforts are needed to identify subtle signs of the intracranial extension during the early course of the disease, which may enable timely initiation of appropriate treatment.
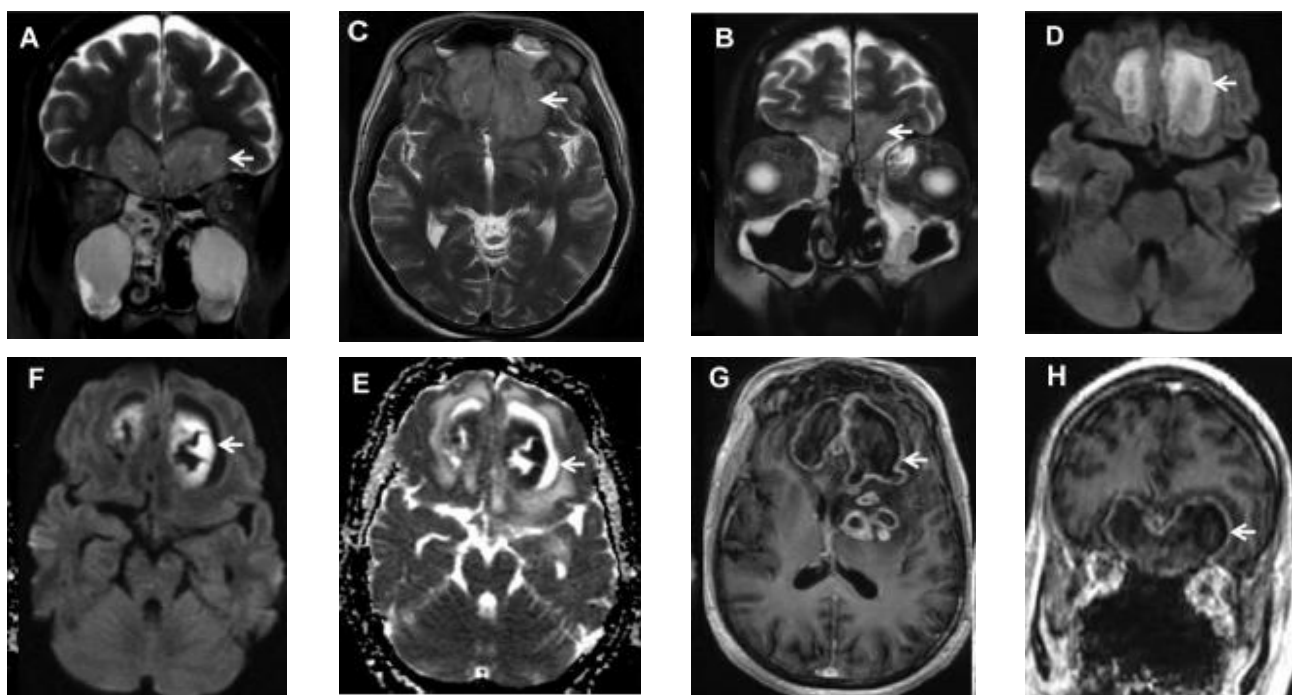

Figure 4. Key imaging features of a complicated stage 3 disease in 56-year-old man who recovered from coronavirus disease 2020 (COVID-19) 15 days previously and presented with continuous dull aching frontal headache, left facial numbness, loss of smell, and retro-orbital pain for the past 7 days. He was treated and discharged 5 days back from the hospital with moderate COVID-19 pneumonia and a computed tomography (CT) severity score of 13 of 25. He had known hypertension and diabetes and had been taking on oral hypoglycemic agents for the past 12 years and was treated briefly with supplementary oxygen and steroids for 12 days during hospitalization. Top row: Coronal and axial T2-weighted fat-suppressed images (AeC) show hyperintense lesions involving the both medial basifrontal lobes with diffusion restriction (D) representing cerebritis (arrows). Bottom row: Disease progression is noted during next 10 days despite adequate medical management, resulting in typical fungal cerebral abscess characterized by irregular peripheral projections (arrows), which are showing restricted diffusion and peripheral enhancement (EeH). Also note the perilesional edema and left basal ganglionic multiple small abscesses showing peripheral enhancement (G).

We contextualize the spectrum of the imaging findings observed in this study of COVID-19eassociated ROCM from a pathophysiologic perspective. Cerebritis or brain abscess is a severe complication and occurs either due to the direct spread from the adjacent paranasal sinuses or via a hematogenous route. Fungal abscesses show diffusion restriction along the wall with intracavitary projections and sparing the core of the lesion (Figure 5) [3]. As regards stroke, free iron in the blood and tissue plays a major role in vascular invasion [15]. Endothelial injury by severe acute respiratory syndrome coronavirus 2 infection along with the dysregulated immune response also may be contributing to the arterial involvement resulting in both ischemic strokes as well as aneurysms and hemorrhage [16]. Internal carotid artery invasion is possible either by direct invasion or through retrograde spread from the ophthalmic artery. Posterior circulation stroke occurs due to basilar system involvement (Figure 5) possibly by retrograde perineural spread or direct invasion after skull base osteomyelitis. Mycotic aneurysms are seen as variable-sized irregular outpunching on time-of-flight magnetic resonance angiography source images. Diffusion-weighted imaging helps in detecting early ischemia/infarction.

Venous involvement leads to thrombosis or thrombophlebitis also has been observed. Cavernous sinus involvement may result in thrombosis and/or ophthalmoplegia [16,17]. Our study has several limitations. The retrospective nature of this work and the potential referral bias may have influenced the relatively higher percentages of patients assigned under imaging stage 3.
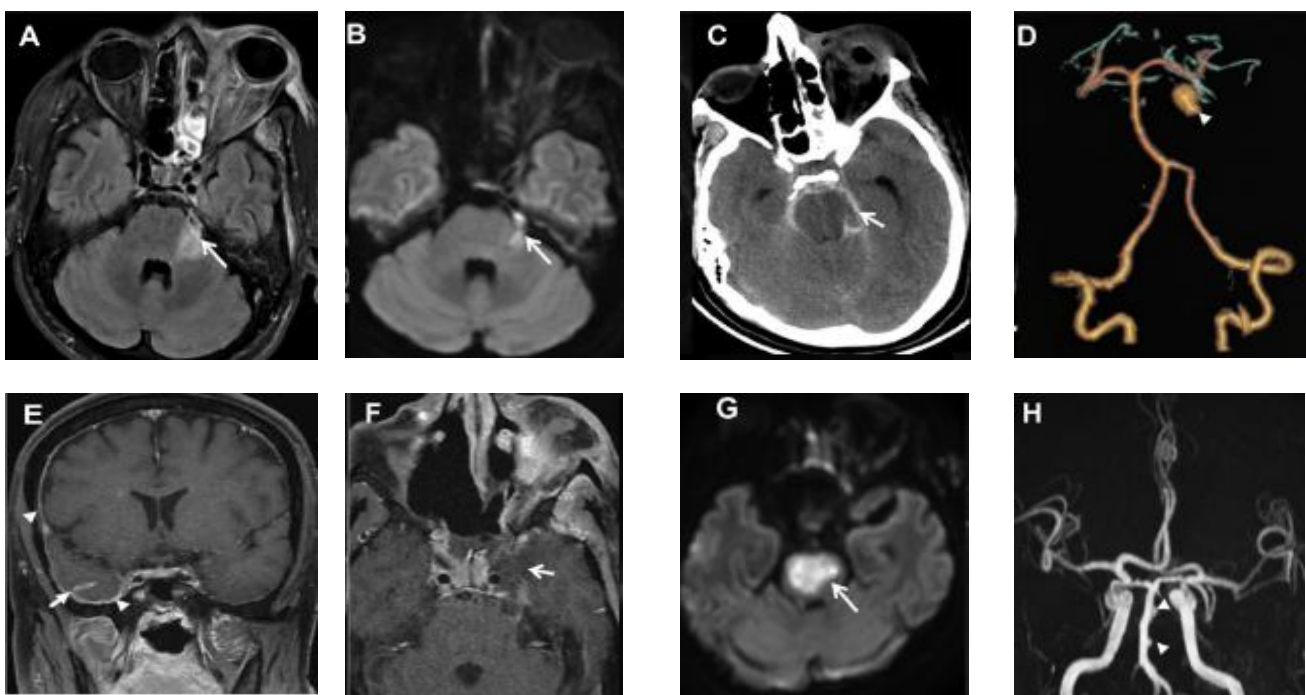

Figure 5. Top row: Key imaging features of complicated stage 3 disease in a 36-year-old man, having recovered from coronavirus disease 2020 (COVID-19) 22 days previously. He was treated and discharged from hospital with moderate COVID-19 pneumonia and computed tomography (CT) severity score of 10 of 25. He had functional endoscopic sinus surgery and orbital exenteration, following which he was doing well for 3 days and on day 4 was found in altered sensorium and succumbed to the illness next day. (AeB) Axial fluid-attenuated inversion recovery and axial diffusion-weighted imaging (DWI) shows thickening of the cisternal portion of left trigeminal nerve and bright signal on DWI (arrows). Note the extensive involvement of left orbit. (C) Axial noncontrast CT shows acute subarachnoid hemorrhage in the basal cisterns (arrow) with early hydrocephalus. (D) CT angiogram volume-rendered image showing large saccular mycotic aneurysm arising from the left superior cerebellar artery (arrowhead). Bottom row: Key imaging features of complicated stage 3 disease in a 46-year-old man, recovered from COVID-19 7 days previously and presented with holocranial headache, left hemi-facial pain, and stuttering right hemiparesis progressing to a locked-in state in next 12 hours. He succumbed to illness the following day. He was initially treated and discharged from the hospital with moderate COVID-19 pneumonia and CT severity score of 14 of 25. (E) Postcontrast T1-weighted (TW1) coronal fat-suppressed postcontrast images showing right-sided pachymeningeal (arrowheads) and leptomeningeal contrast enhancement (arrow). (F) Postcontrast T1W axial fat-suppressed image showing asymmetrical enlargement of left cavernous sinus with poor contrast enhancement (arrows) and thickened cisternal segment of left trigeminal nerve (arrowhead). (G) Axial DWI shows a large pontine acute ischemic infarct (arrow). (H) Coronal time-of-flight magnetic resonance angiography image shows multiple irregular outpouchings from the basilar arterial trunk (arrowheads).

Conclusions. To conclude, we describe the imaging findings of ROCM associated with COVID19 by employing an adapted simplified (3-stage) staging system that can be readily employed in day-to-day practice and help standardize and improve communication between radiologists and clinicians. Disease severity ranges from isolated involvement of sinuses to extensive involvement of the brain. The clinical outcomes of patients with COVID-19 with ROCM progressively scale alongside the graded severity on imaging. This is a rapidly evolving infection with high morbidity and mortality; hence, an early diagnosis of ROCM is crucial, with imaging playing a key role in the staging of the disease process and assessing the involvement of deeper structures that may not be evident clinically. While both CT and MRI are useful, contrastenhanced MRI is the investigation of choice and helps in mapping out the disease extent, particularly with regards to deep facial, orbital and intracranial spread.

Literature:

1. Petrikkos G, Skiada A, Lortholary O, Roilides E, Walsh TJ, Kontoyiannis DP. Epidemiology and clinical manifestations of mucormycosis. Clin Infect Dis. 2012;54(suppl 1):S23-S34.

2. Mehta S, Pandey A. Rhino-orbital mucormycosis associated with COVID-19. Cureus. 2020;12.

3. Mazzai L, Anglani M, Giraudo C, Martucci M, Cester G, Causin F. Imaging features of rhinocerebral mucormycosis: from onset to vascular complications. Acta Radiol. 2022;63:232-244.

4. Sarkar S, Gokhale T, Choudhury SS, Deb AK. COVID-19 and orbital mucormycosis. Indian J Ophthalmol. 2021;69:1002-1004.

5. Singh AK, Singh R, Joshi SR, Misra A. Mucormycosis in COVID-19: a systematic review of cases reported worldwide and in India. Diabetes Metab Syndr. 2021;15:102146.

6. Safder S, Carpenter JS, Roberts TD, Bailey N. The "black turbinate" sign: an early MR imaging finding of nasal mucormycosis. Am J Neuroradiol.2010;31:771-774.

7. Han Q, Escott EJ. The Black Turbinate Sign, A potential diagnostic pitfall: evaluation of the normal enhancement patterns of the nasal turbinates.Am J Neuroradiol. 2019;40:855-861.

8. Khazratov, A. I., Rizaev, J. A., Lisnychuk, N. Y., Reimnazarova, G. D., Kubaev, A. S., & Olimjonov, K. J. (2021). Morphofunctional Characteristics Of The Oral Mucosa Of Experimental Rats In Experimental Carcinogenesis. European Journal of Molecular and Clinical Medicine, 8(2), 227-235.

9. Indiran V. "Guitar pick sign" on MRI. Indian J Ophthalmol. 2019;67:1737.

10. Rizaev J. A., Khaidarov N. K., Abdullaev S. Y. Current approach to the diagnosis and treatment of glossalgia (Literature review) // World Bulletin of Public Health. – 2021. – Т. 4. – С. 96-98.

11. Rizaev J. A., Rizaev E. A., Akhmadaliev N. N. Current view of the problem: A new approach to COVID-19 treatment // Indian Journal of Forensic Medicine & Toxicology. – 2020. – Т. 14. – №. 4. – С. 7341-7347.

12. Rizaev J. A., Maeda H., Khramova N. V. Plastic surgery for the defects in maxillofacial region after surgical resection of benign tumors //Annals of Cancer Research and Therapy. – 2019. – Т. 27. – №. 1. – С. 22-23.

13. Rizaev J. A., Kuliev O. A. Risk factors of anemia in children and prognosing of it // Электронный инновационный вестник. – 2018. – №. 4. – С. 62-65.

14. Rizaev J. A., Shodmonov A. A. Optimization of the surgical stage of dental implantation based on computer modeling //World Bulletin of Public Health. – 2022. – Т. 15. – С. 11-13.

15. Rizaev J. A., Bekmuratov L. R. Prevention of tissue resorption during immediate implant placement by using socket shield technique // Art of Medicine. International Medical Scientific Journal. – 2022. – Т. 2. – №. 3.

16. Rizaev J. A. et al. Peculiarities of the Dynamics of Morbidity of allergic Diseases among Children of Tashkent // Annals of the Romanian Society for Cell Biology. – 2021. – С. 15309-15319.

17. Rizaev J. A. Features of the aggressive forms of periodontitis course // International Journal of Bio-Science and Bio-Technology. – 2019. – Т. 11. – №. 7. – С. 10-16.

КТ И МРТ ДИАГНОСТИКА РИНООФТАЛЬМОЦЕРЕБРАЛЬНОГО МУКОРМИКОЗА У ПАЦИЕНТОВ ПЕРЕНЕСШИХ COVID-19

Абдашимов З.Б., Ходжибекова Ю.М., Юнусова Л.Р.

Резюме. *Риноофтальмоцеребральный мукормикоз (РОЦМ) приобрел масштабы эпидемии, вызвав новую проблему здравоохранения в мире. РОЦМ, ангиоинвазивная инфекция, вызывается нитевидными грибами семейства Micoraceae. Предрасполагающие факторы включают неконтролируемый диабет, гематологические злокачественные новообразования, трансплантацию солидных органов и стволовых клеток, применение кортикостероидов и ослабленный иммунитет. Во время пандемии COVID-19 в Узбекистане значительно увеличилось число пациентов с мукормикозом. РОЦМ преимущественно наблюдается у пациентов с сахарным диабетом/преддиабетом, у которых инфекция COVID-19 увеличивает риск осложнений и летального исхода. Компьютерная томография (КТ) при РОЦМ играет относительно меньшую роль по сравнению с магнитно-резонансной томографией (МРТ), которая в целом обладает лучшим разрешением мягких тканей для оценки распространения заболевания.*

Ключевые слова: *риноофтальмоцеребральный мукормикоз, КТ, МРТ, COVID-19.*